



Contents lists available at ScienceDirect

Steroids

journal homepage: www.elsevier.com/locate/steroids

C₂₁ steroidal glycosides from *Cynanchum stauntonii* induce apoptosis in HepG2 cells

Zhi-Qi Yin^{a,*}, Shu-Le Yu^{a,b,1}, Yu-Jian Wei^c, Lin Ma^{a,b}, Zheng-Feng Wu^{a,b}, Lei Wang^d, Qing-Wen Zhang^e, Ming Zhao^f, Wen-Cai Ye^d, Chun-Tao Che^f, Jian Zhang^{b,*}

^a Department of Natural Medicinal Chemistry & State Key Laboratory of Natural Medicines, China Pharmaceutical University, Nanjing 210009, China

^b Laboratory of Translational Medicine, Jiangsu Province Academy of Traditional Chinese Medicine, Nanjing 210028, China

^c The First Clinical Medical Institute, Nanjing Medical University, Nanjing 210000, China

^d Institute of Traditional Chinese Medicine and Natural Products & Guangdong Province Key Laboratory of Pharmacodynamic Constituents of Traditional Chinese Medicine and New Drugs Research, Jinan University, Guangzhou 510632, China

^e State Key Laboratory of Quality Research in Chinese Medicine and Institute of Chinese Medical Sciences, University of Macau, Macao SAR, China

^f Department of Medicinal Chemistry and Pharmacognosy, and WHO Collaborating Center for Tradition Medicine, College of Pharmacy, University of Illinois at Chicago, Chicago, IL 60612, USA

ARTICLE INFO

Article history:

Received 10 August 2015

Received in revised form 27 November 2015

Accepted 10 December 2015

Available online xxxxx

Keywords:

Cynanchum stauntonii

C₂₁ steroidal glycoside

Apoptosis

Caspase

ABSTRACT

Two new (1–2) and three known (3–5) C₂₁ steroidal glycosides were isolated from *Cynanchum stauntonii*. Their structures were elucidated on the basis of 1D and 2D-NMR spectroscopic data as well as HRTOFMS analysis. The cytotoxicity of the compounds against A549, HepG2, and 4T1 cell lines were evaluated by MTT assay. Compound 4 exhibited good inhibitory activities with the IC₅₀ values 26.82, 12.24, and 44.12 μM, respectively. Furthermore, compound 4 could induce G1 phase arrest, upregulate the expression levels of caspases-3, -9, and Bax, and downregulate the expression level of Bcl-2. These results indicated that compound 4 might be valuable to anticancer drug candidates.

© 2015 Elsevier Inc. All rights reserved.

1. Introduction

Apoptosis, first demonstrated by Kerr in 1972 [1], is mediated by genes resulting in orderly cell death to maintain the stability of the environment in the body, also referred to as 'programmed cell death' or 'cell suicide' [2]. There are extrinsic and intrinsic signaling pathways [3], the former is mediated by death receptor on the cell membrane, activating caspase-8, -10 [4]; the latter works by activating caspase-9, which is regulated by gene family Bcl-2 [5]. Generally, both ways can lead to the activation of caspase-3, DNA fragmentation, and finally cell death [6].

Tumor cells can be eliminated by a number of alternative mechanisms including necrosis and apoptosis, which can be the

therapeutic strategies for cancers [7]. However, necrosis is typically described as a 'nonspecific' form of cell death, with consequent injury to surrounding cells and tissues [8]. By contrast, apoptotic cell removal is more efficient and non-inflammatory [9]. Given the above reasons, more and more studies were focused on the tumor cell apoptosis, in order to achieve good control of cancer while with limited detriment to normal cell function.

In recent years, C₂₁ steroidal glycosides have been receiving increasing attentions because of their bioactivities, including anti-tumor effects. Extensive evidences confirmed that many C₂₁ steroidal glycosides resist cancer by inducing apoptosis [10–15]. *Cynanchum stauntonii* is a perennial herb belonging to the genus *Cynanchum* in the family Asclepiadaceae. It has been reported to be rich in C₂₁ steroidal glycosides. Cytotoxicity evaluation showed that glaucogenin C-mono-D-thevetoside and neocynapanogenin F-mono-D-thevetoside had obvious cytotoxicity in HeLa and Bel-7402 cell lines, respectively [16]. However, there are few reports about the cytotoxicity of C₂₁ steroidal glycosides from *C. stauntonii*, and the potential mechanism is also not clear.

In the present report, we describe the investigation of the C₂₁ steroidal glycosides from *C. stauntonii*, activity evaluation against

* Corresponding authors at: Department of Natural Medicinal Chemistry & State Key Laboratory of Natural Medicines, China Pharmaceutical University, No. 24, Tongjiqiang, Gulou District, Nanjing 210009, Jiangsu Province, China (Z.-Q. Yin). Laboratory of Translational Medicine, Jiangsu Province Academy of Traditional Chinese Medicine, No. 100, Shizi Street, Hongshan Road, Nanjing 210028, Jiangsu Province, China (J. Zhang).

E-mail addresses: cpu-yzq@cpu.edu.cn (Z.-Q. Yin), zjwonderful@hotmail.com (J. Zhang).

¹ These two authors contributed equally to this work.

A549, HepG2 and 4T1 cell lines, as well as the possible mechanism of inducing apoptosis.

2. Experimental

2.1. General methods

IR spectra were recorded on a Nicolet Impact 410 spectrophotometer. UV spectra were recorded using a UV-2500PC spectrometer (Shimadzu, Japan). Optical rotations were measured with a JASCO-1020 polarimeter. ^1H and ^{13}C NMR spectra were obtained on a Bruker Avance-300 (^1H NMR 300 MHz, ^{13}C NMR 75 MHz) and Bruker Avance-500 (^1H NMR 500 MHz, ^{13}C NMR 125 MHz). The HR-ESI-MS analysis were performed on a SynaptTM Q-TOF (Waters, USA). ESI-MS spectra were measured on a HP-1100 LC/EST spectrometer. Silica gel (100–200 mesh, 200–300 mesh, Qingdao Marine Chemical Group Co., China) and Sephadex LH-20 (Pharmacia, Sweden) were employed for column chromatography. All of the solvents and materials were of reagent-grade and purified as required.

2.2. Plant material

The whole fresh plants of *C. stauntonii* were collected in Hubei, China in September 2013, and authenticated by Prof. Minjian Qin (China Pharmaceutical University). A voucher specimen (No. 20130911) was deposited in the herbarium of China Pharmaceutical University, Nanjing, China.

2.3. Extraction and Isolation

The air-dried whole fresh plant of *C. stauntonii* (10 kg) was powdered and refluxed with 80% EtOH (3 × 10 L) for three times to yield a semi-solid residue (450 g). The extract was dispersed in H₂O, partitioned with EtOAc (3 × 5 L) and *n*-BuOH (3 × 5 L), to afford EtOAc fraction (130 g), *n*-BuOH fraction (210 g), and aqueous fraction (110 g), respectively. The EtOAc fraction was subjected to a silica gel column (100 × 8 cm) eluted with a gradient system of CH₂Cl₂–MeOH (50:1 → 0:1, 2 L each), to yield fraction A (52.3 g), B (12.7 g), C (10.4 g), and D (11.9 g). Fraction A was further subjected to silica gel (50 × 8 cm) eluted with petroleum ether–EtOAc (20:1 → 1:1, 1 L each), followed by a Sephadex LH-20 CC (eluted with MeOH) and RP-HPLC (210 nm, MeOH:H₂O, 80:20, 10.0 mL/min) to afford compounds **1** (14.1 mg, *t*_R 38.5 min), **3** (903 mg, *t*_R 15.6 min), and **4** (53.2 mg, *t*_R 82.5 min). Fraction B was chromatographed on a silica gel column (50 × 8 cm) eluted with CH₂Cl₂–MeOH in gradient (50:1 → 0:1, 1 L each), then a Sephadex LH-20 CC (MeOH) and purified by RP-HPLC (210 nm, MeOH:H₂O, 82:18, 10.0 mL/min) to afford compounds **2** (31.5 mg, *t*_R 32.1 min), and **5** (28.6 mg, *t*_R 58.5 min).

2.3.1. Compound 1

Compound **1**: white powder; $[\alpha]_{\text{D}}^{20} + 18.1$ (c 0.015, MeOH); UV (MeOH) λ_{max} : 205, 284 nm; IR ν_{max} cm⁻¹: 3443, 2936, 1734, 1652, 1453, 1386, 1165, 1073; ^1H NMR and ^{13}C NMR (CD₃OD) data see Tables 1 and 2; HR-TOF-MS *m/z*: 685.3009 [M+Cl]⁻ (calcd. for C₃₄H₅₀O₁₂Cl, 685.2991).

2.3.2. Compound 2

Compound **2**: white needle crystal; $[\alpha]_{\text{D}}^{20} + 20.1$ (c 0.126, CHCl₃); UV (MeOH) λ_{max} : 240, 273 nm; IR ν_{max} cm⁻¹: 3409, 2932, 1740, 1660, 1437, 1371, 1160, 1063; ^1H NMR and ^{13}C NMR (CDCl₃) data see Tables 1 and 2; HR-TOF-MS *m/z*: 655.2909 [M+Cl]⁻ (calcd. for C₃₃H₄₈O₁₁Cl, 655.2885).

Table 1

^1H and ^{13}C NMR data for aglycone of compounds **1** (CD₃OD, *J* in Hz) and **2** (CDCl₃, *J* in Hz).

Position	1		2	
	$\delta_{\text{C}}^{\text{a}}$	$\delta_{\text{H}}^{\text{b}}$	$\delta_{\text{C}}^{\text{a}}$	$\delta_{\text{H}}^{\text{b}}$
1	37.54	1.07 (m), 2.04 ^c	36.60	1.09 (m), 1.95 (m)
2	30.54	1.68 (m), 1.94 (m)	29.54	1.61 (m), 2.03 ^c
3	79.92	3.52 (m)	78.04	3.57 (m)
4	39.70	1.65 (m), 2.20 (m)	38.89	1.65 (m), 2.20 ^c
5	141.69		140.40	
6	121.31	5.42 (d, 5.1)	120.36	5.38 (d, 4.6)
7	30.85	1.35, 2.00 ^c	29.54	1.23 ^c , 2.06 ^c
8	54.47	1.17	53.05	1.33 ^c
9	41.70	2.43 (m)	40.56	2.44 (m)
10	39.40		38.74	
11	24.62	1.25 ^c , 1.29 ^c	23.77	1.25 ^c , 1.31 ^c
12	29.07	2.04 ^c , 2.45 (m)	28.13	2.04 ^c , 2.44 (m)
13	119.43		118.25	
14	176.99		175.84	
15	68.51	3.72 (m), 4.18 (t, 7.3)	67.70	3.84 (m), 4.15 (m)
16	76.50	5.27 (dd, 9.6, 7.1)	75.23	5.31 (dd, 9.7, 7.7)
17	57.10	3.41 (d, 7.6)	55.90	3.44 (d, 7.86)
18	144.48	6.30 (s)	143.46	6.25 (s)
19	18.33	0.95 (s)	18.10	0.92 (s)
20	115.60		114.06	
21	24.87	1.47 (s)	24.71	1.53 (s)

^a Measured at 75 MHz.

^b Measured at 300 MHz.

^c Overlapped signals.

Table 2

^1H and ^{13}C NMR data for sugars of compounds **1** (CD₃OD, *J* in Hz) and **2** (CDCl₃, *J* in Hz).

Position	1		2	
	$\delta_{\text{C}}^{\text{a}}$	$\delta_{\text{H}}^{\text{b}}$	$\delta_{\text{C}}^{\text{a}}$	$\delta_{\text{H}}^{\text{b}}$
		D-The		D-Canaro
1'	102.39	4.33 (d, 7.6)	98.05	4.57 (dd, 9.6, 1.2)
2'	74.77	3.24 (m)	38.70	1.61 ^c , 2.21 ^c
3'	85.97	3.16 ^c	69.91	3.61 (m)
4'	83.39	3.14 ^c	88.62	2.94 (m)
5'	74.38	3.19 ^c	70.55	3.28 (m)
6'	18.07	1.27 (s)	17.98	1.26 (d, 6.0)
-OMe	60.49	3.63 (s)		
		D-Digit		D-Digit
1''	99.88	4.95 (dd, 8.2, 1.4)	99.36	4.82 (dd, 9.5, 0.8)
2''	39.79	1.65 ^c , 2.00 ^c	37.82	1.83 ^c , 2.33 ^c
3''	69.27	4.00 (m)	68.17	4.10 ^c
4''	72.34	3.19 (m)	72.77	3.38 (m)
5''	70.90	3.77 (m)	69.87	3.87 (m)
6''	18.62	1.25 (s)	17.98	1.33 (d, 6.0)

^a Measured at 75 MHz.

^b Measured at 300 MHz.

^c Overlapped signals.

2.3.3. Anhydrohirundignin-3-O-β-D-monothevetoside (3)

White needle crystal; $[\alpha]_{\text{D}}^{20} - 26.1$ (c 0.126, CH₃OH) [lit. 17: -22.8 (c 0.241, CH₃OH)].

2.3.4. Glaucogenin C-3-O-β-D-monothevetoside (4)

White needle crystal; $[\alpha]_{\text{D}}^{20} + 23.5$ (c 0.126, CHCl₃) [lit. 18: +27.4 (c 0.103, CHCl₃)].

2.3.5. Glaucogenin C-3-O-β-D-cymaropyranosyl-(1 → 4)-β-D-digitoxopyranosyl-(1 → 4)-β-D-thevetopyranoside (5)

White amorphous powder; $[\alpha]_{\text{D}}^{20} + 13.8$ (c 0.126, CH₃OH) [lit. 19: +17.7 (c 1.14, CH₃OH)].

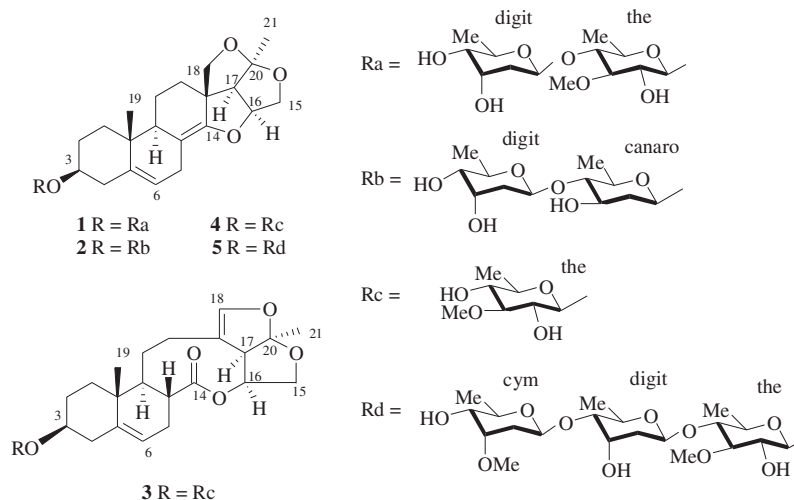


Fig. 1. Chemical structures of compounds 1–5.

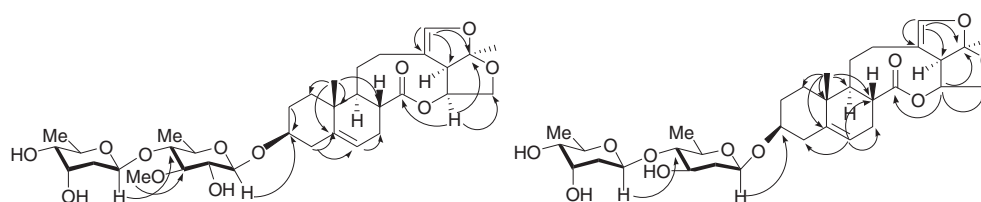


Fig. 2. Key HMBC correlations of compounds 1 (left)-2 (right).

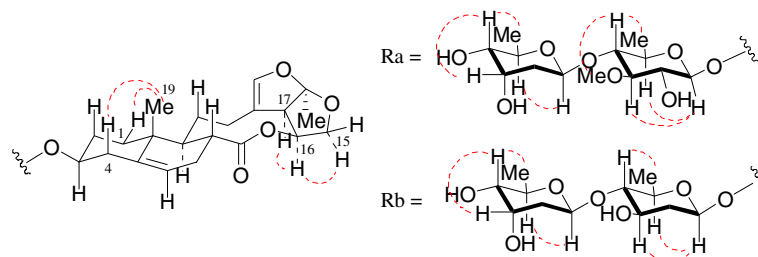


Fig. 3. Key NOESY correlations of compounds 1–2.

Table 3
Cytotoxicity of compounds 1–5 on three tumor cells.

Cell lines	IC ₅₀ 1 ^a	2 ^a	3 ^a	4 ^a	5 ^a
4T1	Ns ^b	Ns	Ns	44.12	Ns
A549	Ns	Ns	Ns	26.82	Ns
HepG2	Ns	Ns	Ns	12.24	Ns

^a μM.

^b Not significant: >100 μM.

2.4. Acid hydrolysis of compounds 1–2

The glycosides (500 mg) were hydrolyzed within MeOH (50 mL) at 60 °C for 5 h, and 0.05 M H₂SO₄ (50 mL). Then the mixture was neutralized with saturated Ba(OH)₂ in H₂O. After the precipitate was removed by filtration, the filtrate was partitioned with CHCl₃. The aqueous layer was concentrated and separated by silica gel CC eluting with CHCl₃–MeOH (8:1, v/v) and then further fractionated by RP-18 CC using a stepwise gradient of MeOH–H₂O (6:4, 7:3 and

8:2, v/v) to give the monosaccharides, D-digitoxose (9 mg), D-canarose (3 mg) and D-thevetose (7 mg), respectively. The specific rotation of these sugars was determined and compared to the literature values for $[\alpha]_D^{20} + 43.5$ (c 0.25, H₂O) for D-digit (lit 20, 21:+45), +25 (c 0.10, H₂O) for D-canaro (lit 20, 21:+22.8) and +55 (c 0.43, H₂O) for D-the (lit 22:+42.3).

2.5. Cell cytotoxicity assay

2.5.1. Cell lines and cell culture

Human lung cancer cells A549, human liver cancer cells HepG2 and rat breast cancer cells 4T1, were obtained from BD (USA). The cell lines were cultured in medium (RPMI1640) with 10% FBS at 37 °C in a humidified incubator with 5% CO₂.

2.5.2. MTT assay

Briefly, cells were seeded in 96-well plate at a density of 5×10^3 cells/well. After overnight incubation, a serial of compounds 1–5 (0.1, 1, 10, 20, 40, 60, 80, 100 μM) were added to wells (triplicate for each concentration). A blank control (wells without

cells), a negative control (cells treated with culture medium), and a positive control (cells employed cisplatin), were included. After 48 h of incubation, all cells were cultured with MTT (5 mg/mL in PBS) for 4 h. After adding 150 μ L of DMSO, the OD value of each well was determined at a wave length of 490 nm. Relative cell proliferation inhibition rate was calculated using the following equation: rate (%) = $(OD_{\text{control group}} - OD_{\text{experimental group}}) / (OD_{\text{control group}} - OD_{\text{blank group}}) \times 100\%$.

2.5.3. Cell apoptosis analysis

The Annexin V-PI kit was used according to the manufacturer instructions (Bipecc, USA). HepG2 cells (1×10^6) were seeded into 24-well culture plates and the cells were treated with medium overnight, followed by a treatment of compound **4** (0, 1, 10, 20 μ M) and cisplatin (20 μ M). After 48 h of treatment, all cells were analyzed by flow cytometry within 1 h (FACSCalibur, Becton Dickinson, USA).

2.5.4. Cell cycle analysis

Cell cycle analysis was carried out by a flow cytometry (Becton Dickinson FACScanTM, CA, USA). Briefly, HepG2 were seeded, harvested and treated with compound **4** (0, 1, 10, 20 μ M). After

48 h treatment, the cells were washed twice with PBS, fixed in 70% ethanol, then stayed overnight. The samples were finally treated with 1% (v/v) Triton X-100 and 0.01% RNase and stained with 0.05% propidium iodide for 30 min in darkness.

2.5.5. Western blot analysis

Apoptosis related protein analysis was analyzed by western blotting to detect the proteins of caspase-3, -8, -9, Bcl-2, Bax. The control and different concentrations of compound **4** (0, 1, 10, 20 μ M) treated HepG2 were used. Cell lysates were prepared in RIPA lysis buffer (Beyotime Institute of Biotechnology, China) and protein concentrations were determined by using a BCA Protein Assay Kit (Thermo, USA) according to the manufacturer's instructions. Samples containing 50 μ g proteins were electrophoresed on SDS-PAGE, transferred onto PVDF membranes (Millipore, USA) and blocked in 5% non-fat milk. The membranes were subsequently incubated with the corresponding primary antibodies for caspase-3, 8, 9, Bcl-2, and Bax (Abcam, Britain). After washing with TBS-T, the membranes were incubated with the secondary antibody for 1 h. The proteins were visualized using Supersignal West Pico Trial kit (Pierce, USA) and exposed to Kodak X-ray films.

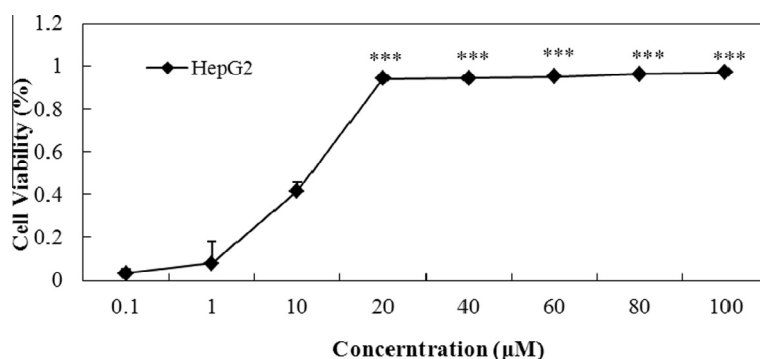


Fig. 4. Compound **4** decreases the cell viability in HepG2. HepG2 cells were treated with different concentrations of compound **4** for 48 h.

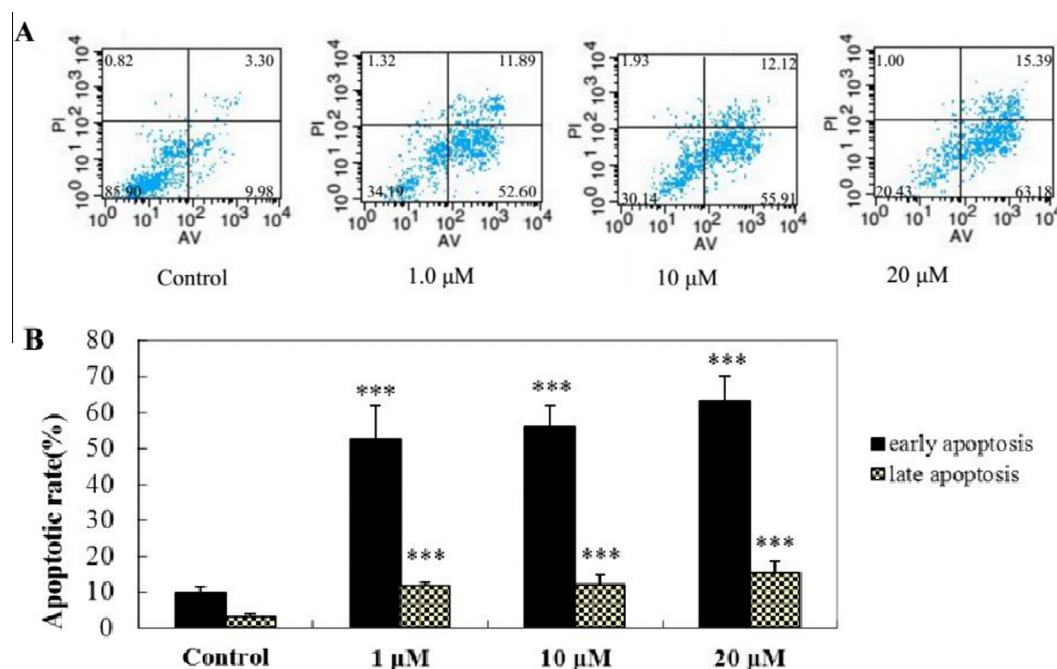


Fig. 5. Compound **4** induces apoptosis in HepG2 cells. (A) The HepG2 cells were treated with different concentrations of **4** for 48 h and the Annexin V/PI assay was used to detect apoptosis using flow cytometry. (B) Representative histograms for apoptotic rate in HepG2 cells.

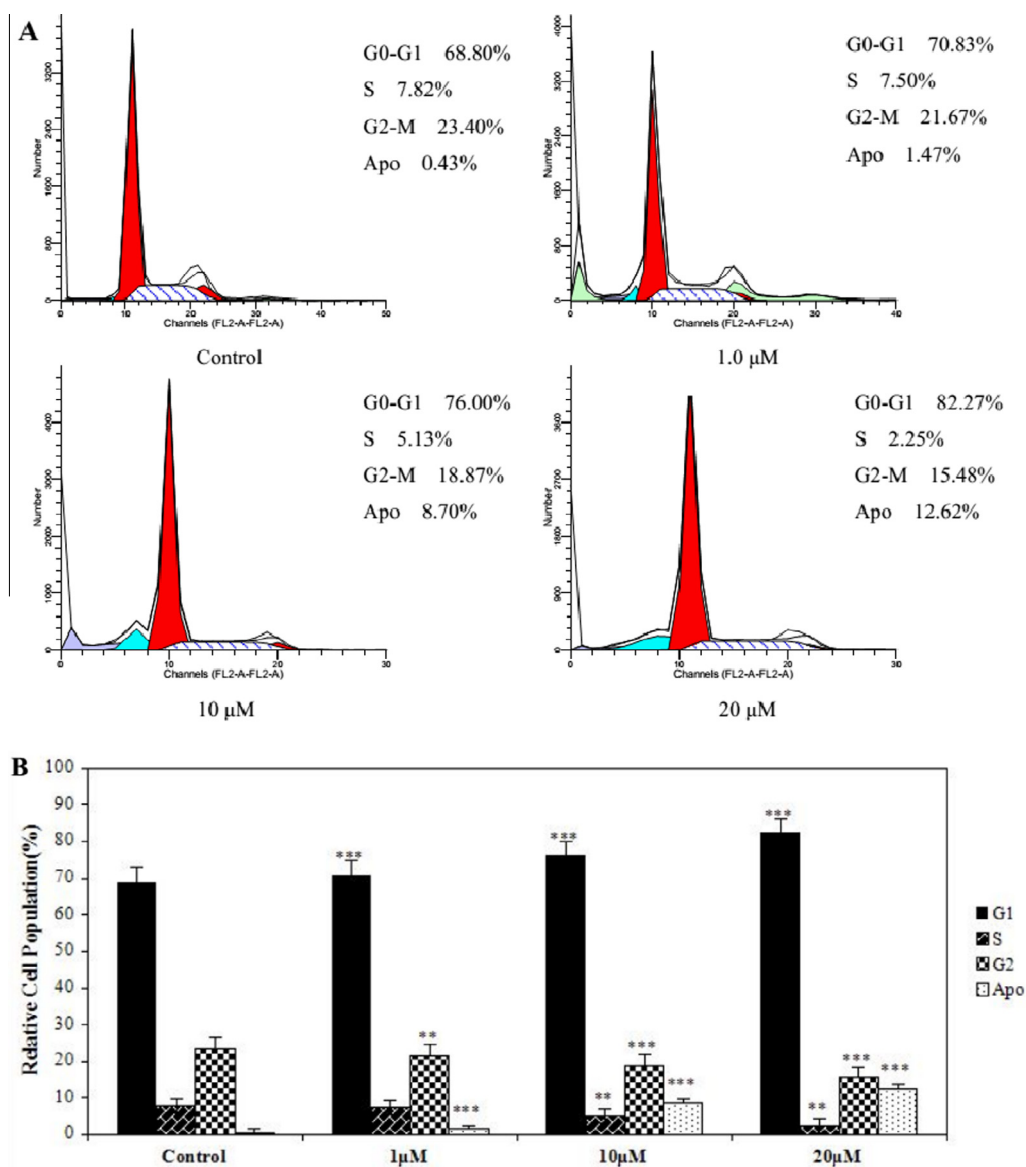


Fig. 6. Compound **4** induced cell cycle arrest at G1 phase in HepG2 cells. (A) HepG2 cells were treated with indicated concentrations of **4** for 48 h. Cell cycle distribution was measured by flow cytometry. (B) Representative histograms for cell cycle distribution in HepG2 cells.

2.6. Statistical analysis

Experimental values were expressed as mean \pm SD. A two-tailed Student's *t*-test was used to examine the significance of the data. A statistically significant difference was considered at $^*P < 0.05$, $^{**}P < 0.01$ and $^{***}P < 0.001$. All calculations were performed using a JMP 5.1 program (SPSS Statistics 17.0 (SPSS Inc., Ireland)).

3. Results and discussion

In this study, two new (**1–2**) and three known (**3–5**) C_{21} steroidal glycosides were identified from *C. stauntonii*. Their anti-proliferation activity and action mechanisms on three cancer cell lines (A549, HepG2 and 4T1) were investigated.

3.1. Structural elucidation of isolated compounds

The 80% EtOH extract of *C. stauntonii* was suspended in H_2O , and partitioned into EtOAc and *n*-BuOH-fractions. Five steroid glycosides (**1–5**) (Fig. 1) were obtained from EtOAc fraction.

Compound **1** was obtained as white powder (CH_3OH). The molecular formula was determined as $\text{C}_{34}\text{H}_{50}\text{O}_{12}$ by HR-TOF-MS (m/z 685.3009 $[\text{M}+\text{Cl}]^-$, calcd for $\text{C}_{34}\text{H}_{50}\text{O}_{12}\text{Cl}$, 685.2991). The IR spectrum exhibited absorptions at 3444 cm^{-1} (hydroxyl), 1734 cm^{-1} (carbonyl) and 1652 cm^{-1} (olefinic). The ^1H NMR spectrum showed characteristic shift values of a aglycone of gluco-genin C-3-*O*- β -*D*-monothevetoside [16] with two olefinic protons at δ_{H} 5.42 (1H, d, $J = 5.1$ Hz), 6.30 (1H, s) and two methyls at δ_{H} 0.95 (3H, s) and 1.47 (3H, s). Furthermore, the ^{13}C NMR spectrum also exhibited the corresponding carbon signals from the aglycone. The ^1H NMR spectrum also displayed signals corresponding to two anomeric protons at δ_{H} 4.33 (d, $J = 7.6$ Hz) and δ_{H} 4.95 (dd, $J = 8.2, 1.4$ Hz), which correlated with the anomeric carbon signals at δ_{C} 102.4 and δ_{C} 99.9 in the ^{13}C NMR spectrum. The NMR data of the sugar units (Table 2) suggested the presence of a digitoxopyranose and a thevetopyranose, and the sugars were believed to be in the D-form on the basis of their optical rotation values. Their anomeric configurations were all determined as β based on their $J_{\text{H}-1',\text{H}-1''}$ coupling constants and the ^{13}C NMR data of the sugar units (Table 2).

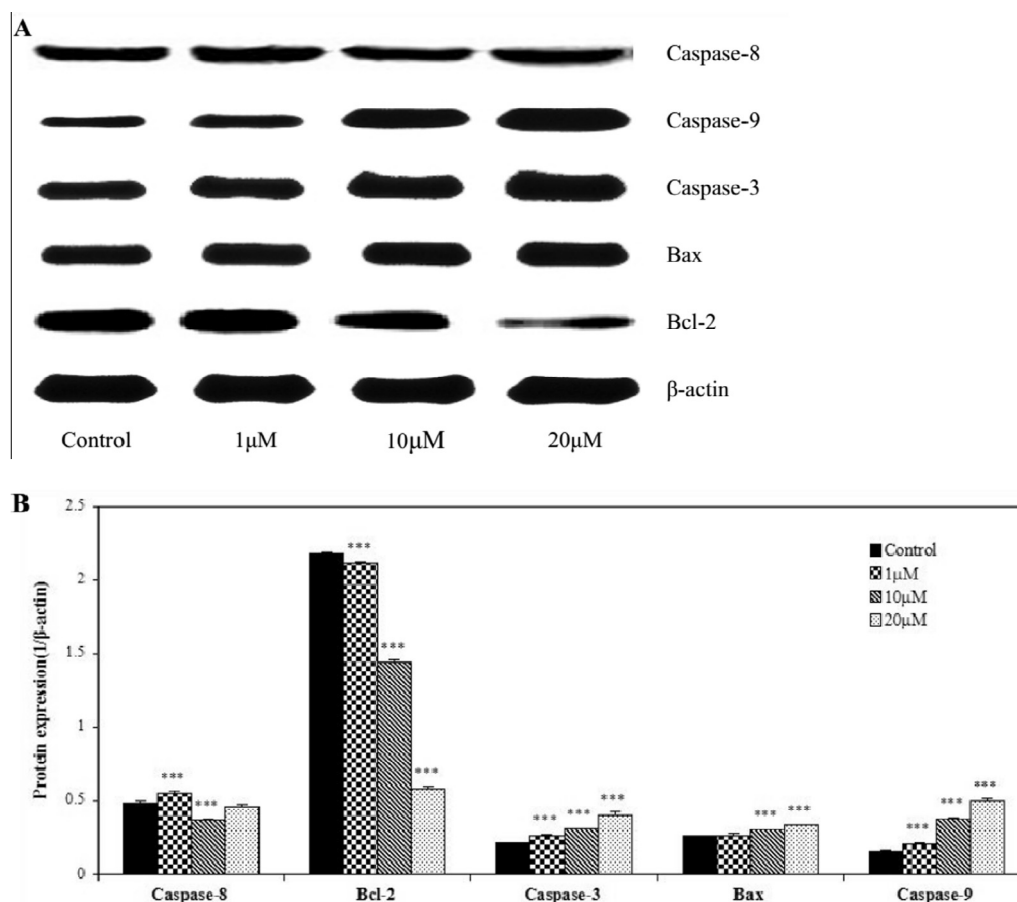


Fig. 7. Effect of compound **4** on protein expressions of apoptosis related genes of HepG2 tumor cells. (A) The protein level of caspase-3, -8, -9, Bax and Bcl-2 was examined by western blot assay, and β -actin was used as a loading control. (B) The histogram shows that there were significant increases of caspase-3, -9, Bax, significant decrease of Bcl-2 in dose-dependent manners after drug treatment.

In the HMBC spectrum, correlations of The-H-1' (δ 4.33) with C-3 (δ 79.9), and Digit-H-1'' (δ 4.95) with The-C-4' (δ 83.4) were observed, indicating the linkage as shown in Fig. 2. In addition, the correlations observed in the NOESY experiment also supported the proposed relative configuration of **1**, in which NOESY correlations of H-19 and H-1 β and H-4 β , of H-16 and H-17 and H-15, H-1' $_{ax}$ and H-3' $_{ax}$ and H-5' $_{ax}$, of H-1'' $_{ax}$ and H-5'' $_{ax}$ indicated the orientation of the aglycone and two sugars (Fig. 3). Thus, the structure of **1** was established as glaucogenin C-3-O- β -D-digitoxopyranosyl-(1 \rightarrow 4)- β -D-thevetopyranoside.

Compound **2** was isolated as white needle crystals (CHCl₃), mp 232–234 °C. The molecular formula was determined as C₃₃H₄₈O₁₁ by HR-TOF-MS at m/z 655.2909 [M+Cl]⁻ (calcd for C₃₃H₄₈O₁₁Cl, 655.2885). The IR spectrum showed the absorptions of 3409 cm⁻¹ (hydroxyl), 1739 cm⁻¹ (carbonyl) and 1660 cm⁻¹ (olefinic). A detailed NMR data comparison of compounds **2** with **1** revealed that they shared the same aglycone moiety. The ¹H NMR spectrum showed the anomeric proton of two 6-deoxysugar at δ_H 4.57 (dd, J = 9.6, 1.2 Hz) and δ_H 4.82 (dd, J = 9.5, 0.8 Hz), which correlated to the corresponding anomeric carbon signals at δ 98.0 and δ 99.4 in the ¹³C NMR spectrum. The ¹H-¹H COSY experiment, combined with the HSQC spectrum, established the connection within the sugar moiety. The presence of a β -D-canaropyranose and a β -D-digitoxopyranose were determined by their optical rotation values, which were also supported by the NOE correlations of H-1' $_{ax}$ and H-3' $_{ax}$ and H-5' $_{ax}$, of H-1'' $_{ax}$ and H-5'' $_{ax}$ in the NOESY spectrum (Fig. 3). The linkage of the two sugars were deduced by the correlations between Canaro-H-1' (δ 4.57) and C-3 (δ 78.0), Digit-H-1'' (δ 4.82) and Canaro-C-4' (δ 88.6) in the HMBC spectrum.

Thus, the structure of compound **2** was determined to be glaucogenin C-3-O- β -D-digitoxopyranosyl-(1 \rightarrow 4)- β -D-canaropyranoside.

Additionally, the known compounds were identified to be anhydrohirundignin-3-O- β -D-monothevetoside (**3**) [17], glaucogenin C-3-O- β -D-monothevetoside (**4**) [16], glaucogenin C-3-O- β -D-cymaropyranosyl-(1 \rightarrow 4)- β -D-digitoxopyranosyl-(1 \rightarrow 4)- β -D-thevetopyranoside (**5**) [19], on the basis of the NMR data comparison.

3.2. Cell cytotoxicity assay

3.2.1. MTT assay

The MTT assay was employed to evaluate the cytotoxicity of compound **1–5** on tumor cells. The results were summarized in Table 3 and Fig. 4. Compound **4** could obviously inhibit the cell growth in a dose-dependent manner, and be most active against HepG2 with a IC₅₀ value of 12.24 μ M, while the IC₅₀ of cisplatin is 21.51 μ M, indicating that HepG2 was slightly more sensitive to compound **4**. Therefore, compound **4** was selected for further mechanism study on HepG2 cell line.

3.2.2. Compound **4** induces apoptosis in HepG2 Cells

Induction of apoptosis and cell cycle arrest are two main ways for cell growth inhibition [23]. Annexin V/PI staining was employed to discriminate among normal cells (Annexin V-/PI-), early apoptotic cells (Annexin V+/PI-), late apoptotic cells (Annexin V+/PI+), and necrosis cells (Annexin V-/PI+). As shown in Fig. 5, compound **4** could increase the number of apoptosis cells in a concentration-dependent manner. After 48 h treatment,

compound **4** at 1 μM caused 52.60% early apoptosis and 11.89% late apoptosis, while 55.91% early apoptosis and 12.12% late apoptosis at 10 μM , 63.18% early apoptosis and 15.39% late apoptosis at 20 μM . These results suggested that the growth inhibitory effect of compound **4** was partly due to apoptosis of HepG2 cells.

3.2.3. Compound **4** induced cell cycle arrest at G1 phase in HepG2 cells

To determine whether the anti-proliferative effect is related to cell cycle arrest, we examined the cell cycle changes after drug treatment. As shown in Fig. 6, compound **4** induced cell cycle arrest at G1 phase. The percentage of cells in G0-G1 phase increased from 68.80% as the control to 82.27% treated at the highest dose (20 μM). Meanwhile, the apoptotic cell rate increased from 0.43% to 12.62%. These were accompanied with a decreased percentage of cells in S and G2-M phase. These results indicated that compound **4** exerted its growth suppressive activity by perturbing cell cycle progression.

3.2.4. Western blot analysis

There are two major signaling pathways in mammalian cells leading to apoptosis: the caspase-8-initiated extrinsic and the caspase-9-dependent intrinsic pathways [24], and caspase-3 is the downstream molecule. The extrinsic pathway is induced by death receptors, the engagement of which can result in aggregation of caspase-8 molecules, incurring their auto-activation. While the intrinsic pathway is triggered by cellular stress, which can induce death-promoting members of the gene family Bcl-2 (e.g. Bid, Bax, Bad) to translocate to mitochondria. This event might facilitate escape of mitochondrial cytochrome *c*, which can be blocked by death-inhibitory members (Bcl-2, Bcl-XL). Cytochrome *c* can combine with Apaf-1 which may promote the recruitment of caspase-9 into a multimeric Apaf-1-caspase-9 complex that results in caspase-9 activation [5]. Caspase-8 and caspase-9 then activate a cascade of further caspase activation events leading to cellular destruction.

To elucidate the molecular mechanisms underlying the induction of apoptosis by compound **4**, we examined the expression of caspase-8, -9, -3, Bax, Bcl-2. The results (Fig. 7) suggested that the levels of caspase-9, -3 and Bax were greatly increased, while Bcl-2 was decreased in all the doses tested, indicating that compound **4** induced apoptosis via a mitochondrial pathway.

Due to the limited quantity of compound **4**, the *in vivo* experiment was not performed yet. To enrich more C_{21} steroidal glycosides for further *in vivo* investigation is just on-going in our lab.

4. Conclusion

Compound **4** could significantly inhibit the cell growth, inducing G1 phase arrest and apoptotic cell death in human liver cancer HepG2 cells *in vitro*. The caspases also participate in this process. The present data provides a scientific support for the potential utilization of *C. stauntonii* as a new source of lead compounds for cancer therapy.

Acknowledgments

The authors thank Prof. Min-Jian Qin (China Pharmaceutical University) for authenticating the plant material and Prof.

Wen-Bin Shen (China Pharmaceutical University) for NMR measurements. This work was partially supported by grants awarded from the National Natural Science Foundation of China (No. 81001379), the Ninth Batch of “Six Talent Peaks” Project of Jiangsu Province (No. 2012-YY-008), and A Project Funded by the Priority Academic Program Development of Jiangsu Higher Education Institutions.

Appendix A. Supplementary data

HRTOFMS and NMR spectra of compounds 1–5 are available as supporting information. Supplementary data associated with this article can be found, in the online version, at <http://dx.doi.org/10.1016/j.steroids.2015.12.008>.

References

- [1] J.F. Kerr, A.H. Wyllie, A.R. Currie, Apoptosis: a basic biological phenomenon with wide-ranging implications in tissue kinetics, *Br. J. Cancer* 26 (1972) 239–257.
- [2] R. Zhang, Y. Liu, Y. Wang, Y. Ye, X. Li, Cytotoxic and apoptosis-inducing properties of auriculoside A in tumor cells, *Chem. Biodivers.* 4 (2007) 887–892.
- [3] D.L. Vaux, A. Strasser, The molecular biology of apoptosis, *Proc. Natl. Acad. Sci. U.S.A.* 93 (1996) 2239–2244.
- [4] H. Walczak, P.H. Krammer, The CD95 (APO-1/Fas) and the TRAIL (APO-2L) apoptosis systems, *Exp. Cell Res.* 256 (2000) 58–66.
- [5] C. Adrain, S.J. Martin, The mitochondrial apoptosome: a killer unleashed by the cytochrome *seas*, *Trends Biochem. Sci.* 26 (2001) 390–397.
- [6] S. Huerta, E.J. Goulet, S. Huerta-Yepez, E.H. Livingston, Screening and detection of apoptosis, *J. Surg. Res.* 139 (2007) 143–156.
- [7] S. Kasibhatla, B. Tseng, Why target apoptosis in cancer treatment?, *Mol. Cancer Ther.* 2 (2003) 573–580.
- [8] G. Kroemer, B. Dallaporta, M. Resche-Rigon, The mitochondrial death/life regulator in apoptosis and necrosis, *Annu. Rev. Physiol.* 60 (1998) 619–642.
- [9] P.M. Henson, D.L. Bratton, V.A. Fadok, Apoptotic cell removal, *Curr. Biol.* 11 (2001) 795–805.
- [10] R.S. Zhang, Y.P. Ye, Y.M. Shen, H.L. Liang, Two new cytotoxic C-21 steroidal glycosides from the root of *Cynanchum auriculatum*, *Tetrahedron* 56 (2000) 3875–3879.
- [11] S.H. Day, J.P. Wang, S.J. Won, C.N. Lin, Bioactive constituents of the roots of *Cynanchum atratum*, *J. Nat. Prod.* 64 (2001) 608–611.
- [12] Y. Li, J. Zhang, X. Gu, Y. Peng, W. Huang, S. Qian, Two new cytotoxic pregnane glycosides from *Cynanchum auriculatum*, *Planta Med.* 74 (2008) 551–554.
- [13] Y.R. Peng, Y.B. Li, X.D. Liu, J.F. Zhang, J.A. Duan, Antitumor activity of C-21 steroidal glycosides from *Cynanchum auriculatum* Royle ex Wight, *Phytomedicine* 15 (2008) 1016–1020.
- [14] H. Bai, W. Li, Y. Asada, T. Satou, Y. Wang, K. Koike, Twelve pregnane glycosides from *Cynanchum atratum*, *Steroids* 74 (2009) 198–207.
- [15] V.P. García, J. Bermejo, S. Rubio, J. Quintana, F. Estévez, Pregnane steroidal glycosides and their cytostatic activities, *Glycobiology* 21 (2011) 619–624.
- [16] M. Zhang, J.S. Wang, J. Luo, D.D. Wei, L.Y. Kong, Glucogenin E, a new C_{21} steroid from *Cynanchum stauntonii*, *Nat. Prod. Res.* 27 (2013) 176–180.
- [17] P. Wang, H.L. Qin, L. Zhang, Z.H. Li, Y.H. Wang, H.B. Zhu, Steroids from the roots of *Cynanchum stauntonii*, *Planta Med.* 70 (2004) 1075–1079.
- [18] N. Takashi, H. Koji, M. Hiroshi, The structures of glucogenin A, glucogenin B, and glucogenin C-mono-D-thevetoside from Chinese drug “Pai-ch’ien” *Cynanchum* (Decne.) Hand.-Mazz. [J], *Tetrahedron Lett.* 23 (7) (1982) 757–760.
- [19] J.Q. Yu, Z.H. Zhang, A.J. Deng, H.L. Qin, Three new steroidal glycosides from the roots of *Cynanchum stauntonii*, *BioMed. Res. Int.* 2013 (2012) 1–7.
- [20] T. Warashina, T. Noro, Steroidal glycosides from the aerial part of *Asclepias incarnata*, *Phytochemistry* 53 (2000) 485–498.
- [21] T. Warashina, T. Noro, Steroidal glycosides from the aerial part of *Asclepias incarnata* L. II, *Chem. Pharm. Bull. (Tokyo)* 48 (2000) 99–107.
- [22] A.I. Hamed, M.G. Sheded, A.E.S.M. Shaheen, F.A. Hamada, C. Piza, S. Piacente, Polyhydroxypregnane glycosides from *Oxystelma esculentum* var. *alpini*, *Phytochemistry* 65 (2004) 975–980.
- [23] B. Ye, J. Yang, J. Li, T. Niu, S. Wang, *In vitro* and *in vivo* antitumor activities of tenacissoside C from *Marsdenia tenacissima*, *Planta Med.* 80 (2014) 29–38.
- [24] I.M. Ghobrial, T.E. Witzig, A.A. Adjei, Targeting apoptosis pathways in cancer therapy, *CA: Cancer J. Clin.* 55 (2005) 178–194.